

Low-Temperature Excitations of Dilute Lattice Spin Glasses

STEFAN BOETTCHER(*)

Physics Department, Emory University, Atlanta, Georgia 30322, USA

PACS. 75.10.Nr – Spin-glass and other random models.

PACS. 05.50.+q – Lattice theory and statistics (Ising, Potts, etc.).

PACS. 02.60.Pn – Numerical optimization.

Abstract. – A new approach to exploring low-temperature excitations in finite-dimensional lattice spin glasses is proposed. By focusing on bond-diluted lattices just above the percolation threshold, large system sizes L can be obtained which lead to enhanced scaling regimes and more accurate exponents. Furthermore, this method in principle remains practical for any dimension, yielding exponents that so far have been elusive. This approach is demonstrated by determining the stiffness exponent for dimensions $d = 3$, $d = 6$ (the upper critical dimension), and $d = 7$. Key is the application of an exact reduction algorithm, which eliminates a large fraction of spins, so that the reduced lattices never exceed $\sim 10^3$ variables for sizes as large as $L = 30$ in $d = 3$, $L = 9$ in $d = 6$, or $L = 8$ in $d = 7$. Finite size scaling analysis gives $y_3 = 0.24(1)$ for $d = 3$, significantly improving on previous work. The results for $d = 6$ and $d = 7$, $y_6 = 1.1(1)$ and $y_7 = 1.24(5)$, are entirely new and are compared with mean-field predictions made for $d \geq 6$.

Introduction. – In this Letter we propose to study low-energy excitations in Edwards-Anderson spin glasses using *bond-diluted* lattices. All previous studies of such excitations have been hampered by less-than-adequate scaling behavior that can be obtained with the limited systems sizes L accessible on undiluted lattices. Consequently, important questions regarding the spin-glass state in finite dimensional systems remain unresolved [1, 2].

A diluted lattice exhibits less frustration on short distances, and it would appear that the trade-off between potentially larger, yet less frustrated lattices should not improve the attainable scaling regime. Here, we find for the case of the ground-state stiffness [3–5] of $\pm J$ spin glasses on diluted hyper-cubic lattices that instead scaling corrections *diminish* with the dilution. Hence, in combination with finite-size scaling, a dramatically increased scaling window is obtained. This improves the value for the stiffness exponent from the previously accepted value of at best $y_3 = 0.2(1)$ [6–8] to our new value of $y_3 = 0.24(1)$, which may make the difference between merely knowing that a positive y_3 exists and potentially using exponents to distinguish theories [2].

As a further benefit, the relevant bond-density regime is located just above the percolation transition, at which the mean connectivity for diluted lattices barely exceeds unity, invariably,

(*) <http://www.physics.emory.edu/faculty/boettcher>

for *any* dimension d . Accordingly, using exact graph reduction methods, we can study excitations in all dimensions with system sizes L that are beyond the scope of undiluted lattices. For instance, reducing lattices with up to 9^6 spins, we obtain an entirely new result for the upper critical dimension $d = 6$, $y_6 = 1.1(1)$. Similarly, using lattices with up to 7^8 spins, we obtain $y_7 = 1.24(5)$, which suggests that the stiffness exponent increases above the upper critical dimension. For results in $d = 4$ and 5 , see Ref. [9].

On one hand, an increase of y_d with d would appear to be consistent with replica theory (RSB) predictions [10]. At least for $d \geq 6$ bulk spins should dominate energy fluctuations induced at the boundary (see Eq. (20) in Ref. [10]), implying $y_d = d\mu$, where μ is the exponent governing energy fluctuations in the (infinite-dimensional) Sherrington-Kirkpatrick model. On the other hand, Ref. [10] also conjectures $\mu = 1/4$, i. e. $y_6^{\text{RSB}} = 1.5$ and $y_7^{\text{RSB}} = 1.75$, well above the results presented here.

Measuring Stiffness. – Stiffness refers to the ability of a spin system in its ordered state to resist the nucleation of domains of overturned spins. The creation of such domains may entail an energetic penalty for forming an interface. The more ordered the state, the higher the energetic barrier and the more “stiff” the resistance. In turn, if the creation of such an interface is accomplished with no or reduced penalty for increasing linear size L of the domain, one may conclude that the system is in a high-temperature state and poses no resistance against fluctuations spreading through the system. Thus, the stiffness exponent y (often labeled θ) is a fundamental quantity to characterize the low-temperature state of a spin glass [3, 11, 12], and its value is frequently relied upon [2, 13]. For instance, Ref. [13] arrives at conclusions excluded by the more precise value presented here.

The stiffness exponent is typically measured via the “defect” energy ΔE of an interface induced in a system of size L by swapping between periodic and anti-periodic boundary conditions along one spatial direction. In a spin glass the interface of such a growing domain can take advantage of already-frustrated bonds to grow at a reduced or even vanishing cost. The width σ of the distribution $P(\Delta E)$ provides a measure for the energetic cost of growing a domain of overturned spins. To wit,

$$\sigma(\Delta E) \sim L^y, \quad (1)$$

where L here refers to the size of a system with an inverted boundary condition. Clearly, it must be $y \leq d - 1$, and a bound of $y \leq (d - 1)/2$ has been proposed for spin glasses [11]. Particularly, ground states of systems with $y \leq 0$ are unstable with respect to spontaneous fluctuations, which can grow at no cost, like in the case of the one-dimensional ferromagnet where $y = d - 1 = 0$. Such a system does not manage to attain an ordered state for any finite temperature. Conversely, a positive y at $T = 0$ indicates a finite-temperature transition into an ordered regime while its value is a measure of the stability of the ordered state.

Due to its importance, there have been many attempts to approximate stiffness exponents in finite-dimensional spin glasses [4–8, 14–18], using transfer matrix, optimization, or renormalization group techniques. It has been argued long ago that $y < 0$ for $d \leq 2$ and $y > 0$ for $d \geq 3$ [4, 6]. Only recently, the stiffness exponent for $d = 2$, below the lower critical dimension, has been determined to considerable accuracy, $y_2 = -0.282(2)$ [16, 17]. There has been little progress for $d \geq 3$, despite significant increases in computational power. In $d = 3$, the accepted value so far has been $y_3 \approx 0.19$ [6, 7], although there have been investigations recently pointing to a larger value, such as 0.23 [8] or 0.27 [16]. All of these studies are based on fitting power-laws over exceedingly narrow scaling windows at relatively small system sizes, $4 \leq L \leq 10$, causing large uncertainties. Our value in $d = 3$ is at the upper end of previous estimates and amazingly close to (but distinct from) the Migdal-Kadanoff prediction, $y_3^{\text{MK}} = 0.25546(3)$ [18].

To understand the shortcomings of previous investigations, it is important to appreciate the complexity of the task: Most numerical studies are based on sampling the variance $\sigma(\Delta E)$ of the distribution of defect energies $P(\Delta E)$ obtained via inverted boundary conditions (or variants thereof [16]). Thus, for an Ising spin glass with periodic boundaries, an instance of fixed, random bonds is generated, its ground-state energy determined, then all bonds within a hyperplane have their sign reversed and the ground-state energy is determined again. The defect energy ΔE is the often-minute difference between those two energies. Many instances of a given size L have to be generated to sample the distribution of ΔE and its width $\sigma(\Delta E)$ accurately. Finally, $\sigma(\Delta E)$ has to be fitted to Eq. (1) for a large and asymptotic range of L .

Even small errors in the energy for either boundary condition, by way of their subtraction, may soon lead to extreme inaccuracies in $P(\Delta E)$. While for $d \leq 2$ efficient algorithms exist to determine ground state energies exactly, and large system sizes can be obtained [16, 17], for $d \geq 3$ no such algorithm exists: The minimization problem is NP-hard [19] with the cost of exact algorithms rising faster than any power of L . Hence, the values quoted previously for y_3 were either based on small systems, $L \leq 4$ [6], or on elaborate heuristic methods with $L \leq 10$ that lead to statistical and systematic errors [7, 8].

Reduction Algorithm. – To overcome those limitations, we propose to increase system size L *without* increasing the optimization problem by considering reduced, bond-diluted lattices. As long as the bond density p is sufficiently above the bond-percolation threshold p_c , the dominant cluster is effectively compact so that the asymptotic scaling behavior expressed in Eq. (1) – and the stiffness exponent y – is *independent* of the bond density p [18, 20]. Furthermore, we have developed a new, exact algorithm, that is capable of drastically reducing the size of sparsely connected spin glass systems, leaving a much reduced graph whose ground state can be approximated with great accuracy.

We will describe the reduction algorithm in more detail elsewhere [21], including its ability to compute the entropy density and overlap for sparse spin glass systems (see also [18]). We focus here exclusively on the reduction rules for the energy at $T = 0$. These rules apply to general Ising spin glass Hamiltonians

$$H = - \sum_{\langle i,j \rangle} J_{i,j} x_i x_j \quad (2)$$

with *any* bond distribution $P(J)$, discrete or continuous, on arbitrary sparse graphs. For convenience, we use a $\pm J$ distribution on bond-diluted hyper-cubic lattices here.

The reductions effect both spins and bonds, eliminating recursively all zero-, one-, two-, and three-connected spins. These operations eliminate and add terms to the expression for the Hamiltonian in Eq. (2), but leave it form-invariant. Offsets in the energy along the way are accounted for by a variable H_o , which is *exact* for a ground state configuration.

Rule I: An isolated spin can be ignored entirely.

Rule II: A one-connected spin i can be eliminated, since its state can always be chosen in accordance with its neighboring spin j to satisfy the bond $J_{i,j}$. For its energetically most favorable state we adjust $H_o := H_o - |J_{i,j}|$ and eliminate the term $-J_{i,j} x_i x_j$ from H .

Rule III: A double bond, $J_{i,j}^{(1)}$ and $J_{i,j}^{(2)}$, between two vertices i and j can be combined to a single bond by setting $J_{i,j} = J_{i,j}^{(1)} + J_{i,j}^{(2)}$ or be eliminated entirely, if the resulting bond vanishes. This operation is very useful to lower the connectivity of i and j at least by one.

Rule IV: Replacing a two-connected spin i between some spins 1 and 2, the graph obtains a new bond $J_{1,2}$, and acquires an offset $H_o := H_o - \Delta H$, by rewriting in Eq. (2)

$$x_i(J_{i,1}x_1 + J_{i,2}x_2) \leq |J_{i,1}x_1 + J_{i,2}x_2| = J_{1,2}x_1x_2 + \Delta H,$$

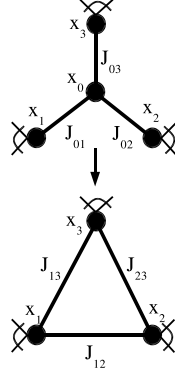


Fig. 1

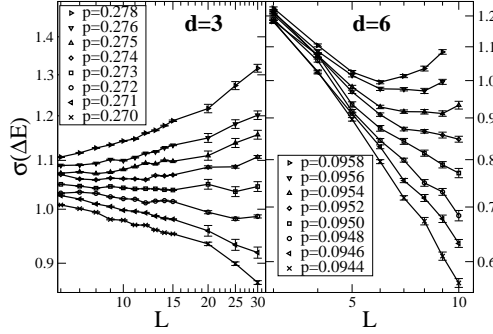


Fig. 2

Fig. 1 – “Star-triangle” relation to reduce a three-connected spin x_0 . The new bonds below are obtained in Eq. (4).

Fig. 2 – Log-log plot of the variance $\sigma(\Delta E)$ of the defect energy as a function of systems size L for various bond fractions $p > p_c$ in $d = 3$ (left) and 6 (right). At small p , $\sigma(\Delta E)$ drops to zero rapidly for increasing L , but turns around and rises for larger p , indicative of a nontrivial ordered state at low T . The longest transients in $\sigma(\Delta E)$ mark p^* , suggesting $p_{d=3}^* = 0.272(1)$ and $p_{d=6}^* = 0.0950(3)$.

$$J_{1,2} = \frac{1}{2} (|J_{i,1} + J_{i,2}| - |J_{i,1} - J_{i,2}|), \quad \Delta H = \frac{1}{2} (|J_{i,1} + J_{i,2}| + |J_{i,1} - J_{i,2}|). \quad (3)$$

Rule V: A three-connected spin i can be reduced via a “star-triangle” relation, see Fig. 1:

$$\begin{aligned} J_{i,1} x_i x_1 + J_{i,2} x_i x_2 + J_{i,3} x_i x_3 &\leq J_{1,2} x_1 x_2 + J_{1,3} x_1 x_3 + J_{2,3} x_2 x_3 + \Delta H, \\ J_{1,2} &= -A - B + C + D, \quad J_{1,3} = A - B + C - D, \quad J_{2,3} = -A + B + C - D, \\ \Delta H &= A + B + C + D, \quad A = \frac{1}{4} |J_{i,1} - J_{i,2} + J_{i,3}|, \\ B &= \frac{1}{4} |J_{i,1} - J_{i,2} - J_{i,3}|, \quad C = \frac{1}{4} |J_{i,1} + J_{i,2} + J_{i,3}|, \quad D = \frac{1}{4} |J_{i,1} + J_{i,2} - J_{i,3}|. \end{aligned} \quad (4)$$

The bounds in Eqs. (3-4) become *exact* when the remaining graph takes on its ground state. Reducing higher-connected spins leads to (hyper-)bonds between multiple spins, unlike Eq. (2).

After a recursive application of these rules, the original lattice graph is either completely reduced (which is almost always the case for $p < p_c$), in which case H_o provides the exact ground state energy already, or we are left with a highly reduced, compact graph in which no spin has less than four connections. We obtain the ground state of the reduced graph with the extremal optimization heuristic [22], which together with H_o provides a very accurate approximation to the ground state energy of the original diluted lattice instance.

Numerical Results. – In Ref. [20] it was shown that spin glasses with a discrete bond distribution on diluted lattices may possess a distinct critical point p^* in their bond density, which is related to the (purely topological) percolation threshold p_c of the lattice *and* the distribution of the bond weights $P(J)$. Clearly, no long-range correlated state can arise below p_c . A critical point distinct from percolation, $p^* > p_c$, emerges when such a correlated state above p_c remains suppressed due to collaborative effects between bonds [20] (see *Rule III*). Thus, to observe any glassy properties on a dilute lattice, we have to ascertain $p > p^*$. In Ref. [18], we were able to locate p^* for the Migdal-Kadanoff lattice, by using the defect energy

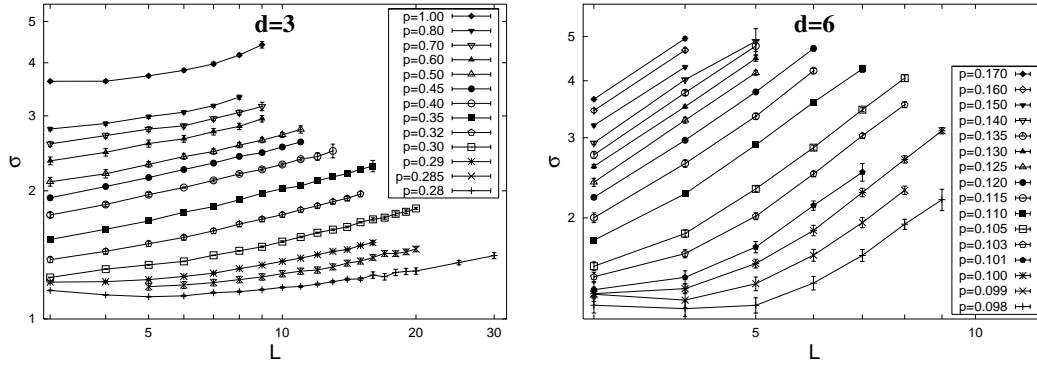


Fig. 3 – Log-log plot of the width σ of the defect energy distribution as a function of system size L for $d = 3$ (top) and 6 (bottom). The data is grouped into sets (connected by lines) parameterized by the bond density p . Most sets show a distinct scaling regime as in Eq. (1) for a range of L above finite scaling corrections but below failing heuristic accuracy.

scaling from Eq. (1): For all $p > p^*$ the stiffness exponent y eventually took on its $p = 1$ value, while for any $p < p^*$ defect energies diminished rapidly for increasing L .

In each dimension (see Ref. [9]), we have run the above algorithm on a large number of graphs (about $10^5 - 10^6$ for each L and p) for p increasing from p_c in small steps. For each given p , L increased until it was clear that $\sigma(\Delta E)$ would either drop or rise for good. In this way, we bracket-in p^* , as shown in Figs. 2 for $d = 3$ and 6 . Tab. I summarizes those results.

While the value of p^* is distribution-dependent, we merely had to establish a bond fraction beyond which we would expect Eq. (1) to hold. Then we can conduct numerical experiments to extract the asymptotic scaling of $\sigma(\Delta E)$ for conveniently chosen p . For each choice of L and p , we have sampled the defect energy distribution with at least $N \geq 10^5$ instances, then determined its variance $\sigma(\Delta E)$. Throughout, the distribution of ΔE is approximately normal, giving rise to an error bar $\propto 1/\sqrt{N}$. In Fig. 3, we plot all the data for each dimension simply according to Eq. (1), on a logarithmic scale. For most sets of graphs, a scaling regime (linear on this scale) is visible. Yet, various deviations from scaling can be observed. Clearly, each sequence of points should exhibit some form of finite size corrections to scaling for smaller L . For large L , the inability to determine defect energies correctly, will inevitably lead to a systematic bias in σ . Some data sets did not exhibit any discernible scaling regime, most notably our set for the undiluted lattice in $d = 3$. This resembles the observation of Refs. [23], which found long transients in similar studies on undiluted $d = 2$ or Migdal-Kadanoff lattices.

To obtain an optimal scaling collapse of the data, we focus on the data inside the scaling regime for each set. To this end, we chose for each data set a lower cut in L by inspection. An appropriate high-end cut is introduced by eliminating all data points for which the remainder graph had a typical size of > 700 spins; at that point the EO heuristic (within the supplied runtime) seems to fail in determining defect energies with sufficient accuracy. All the remaining data points for L and p are fitted to a four-parameter scaling form,

$$\sigma(\Delta E) \sim \mathcal{Y}_0 \left[L (p - p^*)^{\nu^*} \right]^y \quad (L \rightarrow \infty), \quad (5)$$

suggested by Ref. [20]. Unfortunately, we have a-priori no knowledge of corrections for small systems, making the low- L cut on the data a necessity. The fitted values for the fitting constants \mathcal{Y}_0 , ν^* , and y are listed in Tab. I. Using the parameters of this fit, we re-plot only

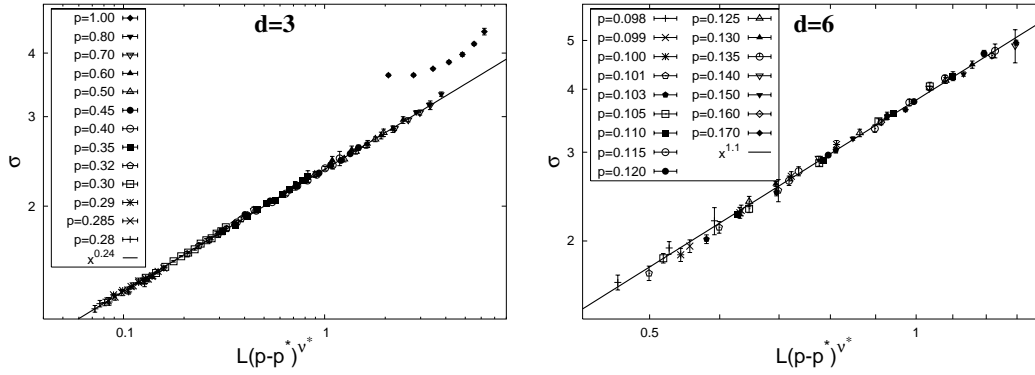


Fig. 4 – Scaling plot of the data from Figs.3 for σ , fitted to the functional form in Eq. (5) as a function of the scaling variable $x = L(p - p^*)^{\nu^*}$ for $d = 3$ (top) and 6 (bottom). Data that fell outside of the scaling regime in each set of Figs. 3 was cut. The straight line in each case represents the fit according to Eq. (5) for the optimal collapse of the data, which provides an accurate determination of the stiffness exponent y in each dimension. For $d = 3$, we have also included the data for $p = 1$, which does not appear to have a scaling regime.

the data from the scaling regime in Figs. 4.

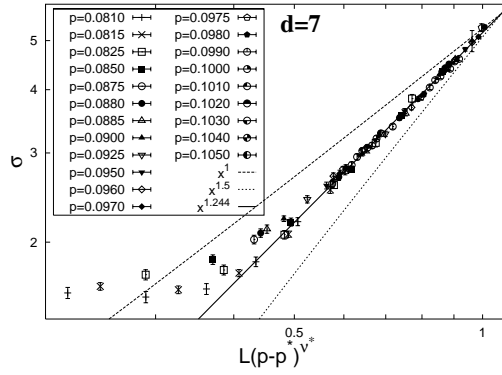
We have also considered the case of $d = 7$. The implementation of our algorithm is not yet capable of handling lattice graphs with much more than 10^6 spins, limiting attainable sizes to $L \leq 8$, which was insufficient to determine p^* directly (as in Fig. 2) as well as the low end of the scaling variable $x = L(p - p^*)^{\nu^*}$. Yet, we have computed about as many data points as for $d = 6$ (see “DoF” in Tab. I), as shown in the scaling plot in Fig. 5. Solid scaling extends over nearly half a decade, yielding $y_7 = 1.24(5)$. Assuming that the data presented in Fig. 5 is asymptotic, any value for y_7 outside of its error bars has a “goodness of fit” Q [24] below 0.001, and $Q < 10^{-100}$ for 1 or 3/2. Generally, y_d appears to be rising with d above the upper critical dimension, but with values and at a rate below replica theory predictions [10].

* * *

I would like to thank A. Percus, F. Krzakala, T. Aspelmeier, and R. Palmer for helpful discussions, and our IT staff for providing access to our student computing lab. This work was supported by NSF grant DMR-0312510.

TABLE I – List of the values for the critical bond-density p^* (from Fig. 2 for $d = 3, 6$), and the fitted values according to Eq. (5) of the correlation-length exponents ν^* , the surface tensions \mathcal{Y}_0 , and the stiffness exponents y , followed by the “goodness of fit,” Q [24], and the degrees of freedom (DoF) used in the fit. Also listed are values for $d = 4$ and 5 from Ref. [9] and the fitted values for $d = 7$.

d	p^*	ν^*	\mathcal{Y}_0	y	$Q(\text{DoF})$
3	0.272(1)	1.17	2.37	0.239	1.00(92)
4	0.1655(5)	0.60	2.43	0.610	0.00(47)
5	0.1206(2)	0.50	3.05	0.876	0.86(48)
6	0.0950(3)	0.44	3.87	1.103	0.02(46)
7	0.080(1)	0.40	5.18	1.244	1.00(55)



S

Fig. 5 – Scaling plot of the data for σ in $d = 7$ dimensions, fitted to the functional form in Eq. (5) as a function of the scaling variable $x = L(p - p^*)^{\nu^*}$. As before, data outside of the scaling regime, although plotted here, was disregarded in the fit. The straight line represents the fit according to Eq. (5) for the optimal collapse of the data. It seems to exclude a simple (half-)integer value for y_7 , such as unity or $3/2$ (dashed lines).

REFERENCES

- [1] KRZAKALA F. and MARTIN O. C., *Phys. Rev. Lett.*, **85** (2000) 3013
- [2] PALASSINI M. and YOUNG A. P., *Phys. Rev. Lett.*, **85** (2000) 3017
- [3] FISCHER K. H. and HERTZ J. A., *Spin Glasses* (Cambridge University Press, Cambridge) 1991
- [4] SOUTHERN B. W. and YOUNG A. P., *J. Phys. C*, **10** (1977) 2179
- [5] KIRKPATRICK S., *Phys. Rev. B*, **15** (1977) 1533
- [6] BRAY A. J. and MOORE M. A., *J. Phys. C*, **17** (1984) L463
- [7] HARTMANN A. K., *Phys. Rev. E*, **59** (1999) 84
- [8] PALASSINI M. and YOUNG A. P., *Phys. Rev. Lett.*, **83** (1999) 5126
- [9] BOETTCHER S., *Euro. Phys. J. B*, **38** (2004) 83
- [10] ASPELMEIER T., MOORE M. A. and YOUNG A. P., *Phys. Rev. Lett.*, **90** (2003) 127202
- [11] FISHER D. S. and HUSE D. A., *Phys. Rev. Lett.*, **56** (1986) 1601
- [12] BRAY A. J. and MOORE M. A., *Phys. Rev. Lett.*, **58** (1987) 57
- [13] BOUCHAUD J.-P., KRZAKALA F. and MARTIN O. C., *Phys. Rev. B*, **68** (2003) 224404
- [14] BANAVAR J. R. and CIEPLAK M., *Phys. Rev. Lett.*, **48** (1982) 832; CIEPLAK M. and BANAVAR J. R., *J. Phys. A*, **23** (1990) 4385; MCMILLAN W. L., *J. Phys. C*, **17** (1984) 3179
- [15] HARTMANN A. K., *Phys. Rev. E*, **60** (1999) 5135
- [16] CARTER A. C., BRAY A. J. and MOORE M. A., *Phys. Rev. Lett.*, **88** (2002) 077201
- [17] HARTMANN A. K., BRAY A. J., CARTER A. C., MOORE M. A. and YOUNG A. P., *Phys. Rev. B*, **66** (2002) 224401
- [18] BOETTCHER S., *Euro. Phys. J. B*, **33** (2003) 439
- [19] BARAHONA F., *J. Phys. A*, **15** (1982) 3241
- [20] BRAY A. J. and FENG S., *Phys. Rev. B*, **36** (1987) 8456
- [21] BOETTCHER S. and PERCUS A. G., (in preparation)
- [22] BOETTCHER S. and PERCUS A. G., *Phys. Rev. Lett.*, **86** (2001) 5211
- [23] DROSSEL B. and MOORE M. A., *Eur. Phys. J. B*, **21** (2001) 589; MIDDLETON A. A., *Phys. Rev. B*, **63** (2001) 060202(R); HARTMANN A. K. and MOORE M. A., *Phys. Rev. Lett.*, **90** (2003) 127201
- [24] PRESS, W. H. , TEUKOLSKY, S. A. , VETTERLING, W. T. and FLANNERY, B. P., *Numerical Recipes in C* (Cambridge Univ. Press, New York) 1992